


Ellipsometric and mechanical characterization of nanostructured anodic oxide film formed on Ti-6Al-7Nb alloy

Luis Felipe N. Guedes¹ · Marcela T. Dalboni Garcia² · Jéssica N. Cunha¹ ·
Lais T. Duarte³ · Denise Bertagnolli^{1,2} · Ladário da Silva^{1,2} · José A. O. Huguenin¹ ·
Elivelton Alves Ferreira¹ 

Received: 2 October 2015 / Revised: 11 January 2016 / Accepted: 25 January 2016 / Published online: 5 February 2016
© Springer-Verlag Berlin Heidelberg 2016

Abstract In this work, we grow TiO₂ nanotube layers by using the single-step direct anodization of Ti-6Al-7Nb alloy in aqueous electrolytes containing F⁻ ions. Nanotube layers are characterized by spectroscopic ellipsometry (SE) and field-emission gun scanning electron microscopy (FEG-SEM). We also use SE to monitor the anodization process for TiO₂ nanotube layers on biocompatible Ti-6Al-7Nb alloy. In addition, we study mechanical properties by nanoindentation.

Keywords Ti-6Al-7Nb alloy · Nanotubes · Ellipsometry · Anodic oxide

Introduction

Nanostructures as nanotubes and nanopores can be formed in anodization processes of valve metals and their alloys accomplished in the presence of fluoride ions. They may present very organized shapes, which resemble self-organized nanostructures [1–6].

The presence of these nanostructures on the surface can alter many properties such as optical ones, hardness, topography, roughness, and of course the available surface area, which is critical for reaction control. Titanium-made materials, in particular, present good biointegration, and if these materials also present surface nanostructures, they could be tailored to alter topography and roughness, key factors for osseointegration [5, 7], in which these materials could then play a major role.

Macak et al. [7] have shown that nanotubes formed on Ti-6Al-7Nb alloy have mainly uniform tubular TiO₂ structures. Rafieerad et al. [8] have observed that the grown TiO₂ nanotube structures were made by a competing mechanism, which included electric field-assisted processes, Ti metal hydrolysis, F⁻ dissociation, and TiO₂ chemical dissolution at the oxide/electrolyte interface. Sungwook Joo et al. [9] have studied the growth processes of anodic TiO₂ nanotube films on Ti by ellipsometry. They have shown that ellipsometry can be used to monitor the “in situ” growth of TiO₂ nanotubes, particularly to control the end point of anodization process. It is worth mentioning that the end point of an anodization process is reached when the nanotube layer dissolution starts.

In the Ti-6Al-7Nb alloy, the non-negligible scatter between individual measurements may be related to the combination of at least two different factors: (i) a different hardness value of the α and β phases, whose contribution would depend on the corresponding β phase/ α phase ratio existing within the tested area in each alloy and (ii) a significant influence of the crystal orientation on the nanoscale mechanical properties [10]. For the Ti-6Al-7Nb alloy, the β phase is partially attacked by NH₄F solution, but the remaining structure also shows a self-organized porous morphology [7]. However, the pore diameter is smaller (about 50 nm in average) than in the α phase.

✉ Elivelton Alves Ferreira
eliveltonalves@id.uff.br

¹ Instituto de Ciências Exatas (ICEx), Universidade Federal Fluminense (UFF), Rua Desembargador Hermydio Ellys Figueira 783, Atarrado, Volta Redonda–RJ CEP 272131-145, Brazil

² Programa de Pós-Graduação em Engenharia Metalúrgica (PPGEM), Universidade Federal Fluminense (UFF), Av. dos Trabalhadores 420-Vila Sta. Cecília, Volta Redonda–RJ CEP 27255-125, Brazil

³ Departamento de Engenharia de Materiais, Centro de Ciências Exatas e de Tecnologia, Universidade Federal de São Carlos (UFSCar), Rodovia Washington Luiz, km 235 Monjolinho, São Carlos-SP, Brazil

Ellipsometry [11] is an indirect and nondestructive technique for examining materials, particularly thin films. It uses the change of the polarization state of the incident light as it interacts with the material in order to access the ellipsometric parameters $\tan(\psi)$ and $\cos(\Delta)$. With the knowledge or hint of the formed structure and with a proper modeling, it is possible to access optical properties of many films in states such as solid, liquid, or gaseous ones. For multiple-layer films, spectroscopic ellipsometry (SE) can be used to characterize “in situ” and “ex situ” film growth. This is particularly interesting as we are studying the anodic growth of nanostructured films on metallic substrates [9, 11, 12].

For osseointegration, nanostructures can also enhance mechanical properties, which are crucial in medical and dental applications. Crawford et al. [13] have reported on an increase of elastic modulus for thinner films of TiO₂ nanotubes on Ti substrate. Investigation of mechanical properties of cement pastes with dispersed nanotubes made using nanoindentation showed that the hardness of the paste can increase or decrease depending on the use of a dispersion agent [14].

The purpose of this paper is to study the mechanical and optical properties of these films with spectroscopic ellipsometry and nanoindentation. Ellipsometry demands the development of an optical model to interpret film behavior in terms of its morphology. Throughout the investigation, optical results will be correlated to FEG-SEM observations of the optically characterized films. A study of hardness and elastic modulus was also performed by nanoindentation.

Experimental

Preparation of the substrate

The material used in this work was obtained from bars of Ti–6Al–7Nb, supplied by Baoji Xinnuo New Metal Materials, China, with chemical composition, microstructure, and tensile mechanical properties in accordance with the requirement of ASTM: F1295-11. The microstructures of the material have a very fine dispersion of α and β phases, without the formation of coarse precipitates at grain boundaries. Further information can be found in Refs. [15, 16]. Prior to anodization, the samples were polished using SiC emery paper (800–2400 grit) and then wet-polished in a diamond slurry.

Anodization of the Ti–6Al–7Nb alloy

Based on the study of anodization of pure titanium [17], we investigated appropriated parameters for anodization of the Ti-alloy. Anodization was performed in a two-electrode electrochemical cell, in which a platinum wire and the specimens were connected to cathode and anode electrodes, respectively. The anodization process was carried out using a direct current

(DC) power source from INSTRUTHERM (model FA-3003) at a constant potential of 20 V for different anodization times. The electrolyte solution was composed of HF and H₃PO₄.

Characterization of TiO₂ nanotube arrays

The morphological features of the nanotubes were characterized by a field-emission gun scanning electron microscope (Quanta-450 FEG). The cross-sectional thickness measurements were carried out by FEG-SEM directly on mechanically cracked and scratched samples.

A spectroscopic ellipsometer from SEMILAB®, model SOPRA GES 5S was used to characterize the growth of oxide films on Ti-6Al-7Nb in “ex situ” experiments. It uses a Xe lamp, with a useful range from 200 to 1000 nm. In our work, we used a wavelength range from 350 to 850 nm, and all measurements were made with an incidence angle of 70° with microspot. The modeling was performed using Spectroscopic Ellipsometry Analyzer (SEA) software from SEMILAB.

The mechanical properties of the nanotubes were probed by nanoindentation, using a Dynamic Ultra-micro Hardness Tester (DUH-211S from Shimadzu®). This technique consists into applying a low-test force on the surface under study by means of an indenter using the electromagnetic loading methods and measuring the indentation depth using a differential transformer. For thin films or a very sensitive coating, a very low force needs to be applied. With DUH 211S, we can reach around 1 μ N. Testing a cycle of loading and unloading charges, it is possible to find dynamical properties as elastic modulus, for example. In our work, we studied dynamical hardness of the nanotubes and compared it with the substrate one. Using a force charge of 2 μ N and Vickers’s indenter, we performed a load and unload test in Ti–6Al–7Nb alloy (substrate) sample and in the sample where we fabricated TiO₂ nanotubes with anodization at 20 V during 20 min.

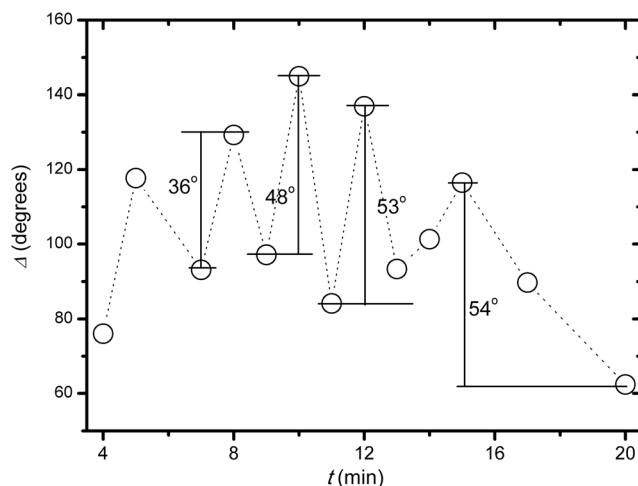


Fig. 1 Changes in the relative phase retardation, Δ , as a function of the anodization time at 546 nm for Ti-6Al-7Nb alloy

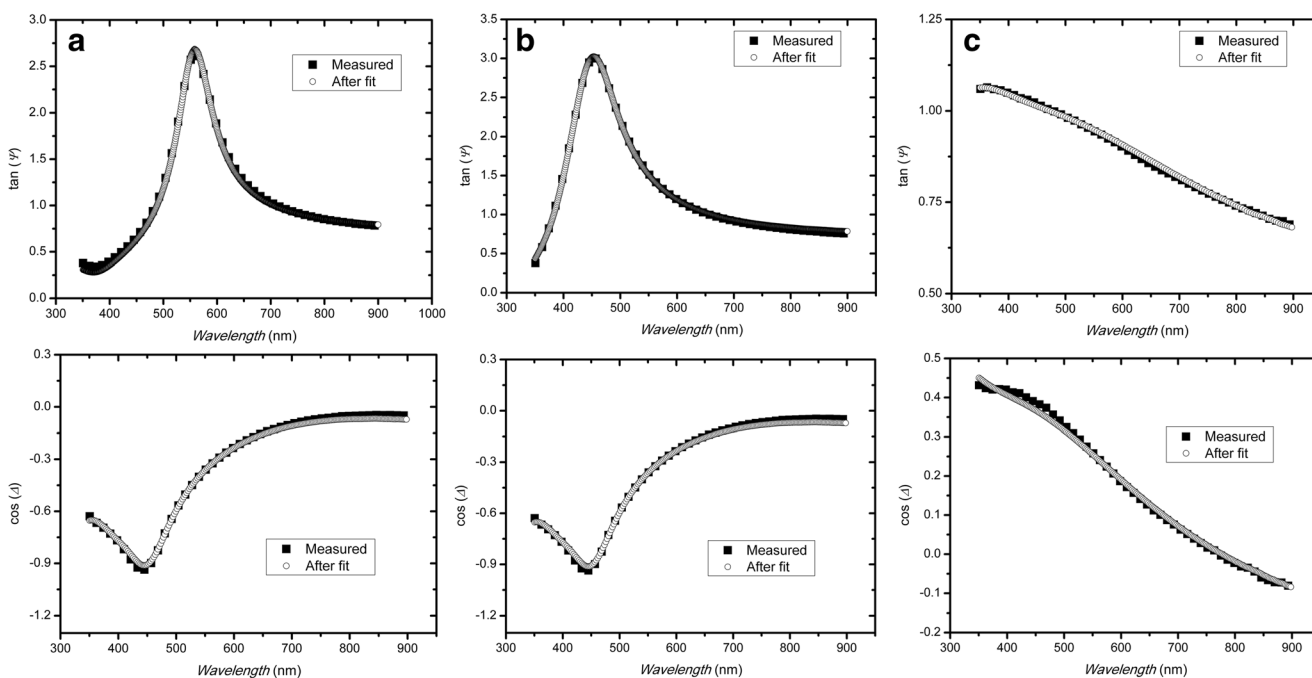


Fig. 2 $\tan(\psi)$ and $\cos(\Delta)$ spectra for nanostructures-type films grown for 2 min (a), 10 min (b), and 20 min (c) and calculated spectra with the model of Fig. 3 for sample (a) and Fig. 4 for samples (b) and (c)

The hold time between the load and unload process was 1.0 s. Dynamical hardness depth indentation and elastic modulus were compared.

To minimize the position dependence of the measured mechanical properties [7, 10], the data presented are the statistical mean values calculated from at least 10 measurements.

Results and discussion

First, we analyze if there is a layer of formed nanotubes on the alloy through the measurements of SE at different times of the anodization. Figure 1 shows changes in Δ at different times, at a wavelength of 546 nm, until 20 min of the anodization of the alloy is reached. The value of Δ undergoes a cyclic change with maxima and minima. The amplitude of this cyclic change in Δ , $\delta\Delta$, is larger than 30° in all cycles indicating that the nanotube layers are growing. As stated by Sungwook et al. [9], when $\delta\Delta$ becomes less than 30° , the dissolution of

nanotubes’ mouths takes place. It is therefore presumed that the oscillations in the Δ vs. t plot indicate nanotube growth. Therefore, as can be seen in Fig. 1, we did not reach the end point of the anodization process. Note that the last angle showed in Fig. 1 is 54° . These SE measurements assure us that we have a structured layer of nanotubes which did not stop growing.

After the verification of the nanotube layer formation from the Δ vs. t plot, we propose optical models for films grown at 2, 10, and 20 min from the SE measurement. The ellipsometry spectra [$\tan(\psi)$ and $\cos(\Delta)$ vs. $wavelength$] for nanostructures-type films grown at 2, 10, and 20 min are shown in Fig. 2a–c, as well as the calculated spectra obtained from modeling.

The model used for films grown for 2 min is shown in Fig. 3. The one used for films grown for 10 and 20 min is presented in Fig. 4. These models have been derived from known optical models [9, 14, 18, 19] and from images of the structure of TiO_2 films on the Ti-6Al-7Nb alloy obtained by

Fig. 3 a Morphology of the rough anodic film after anodization at 20 V for 2 min; b optical model of (a) for SE interpretation

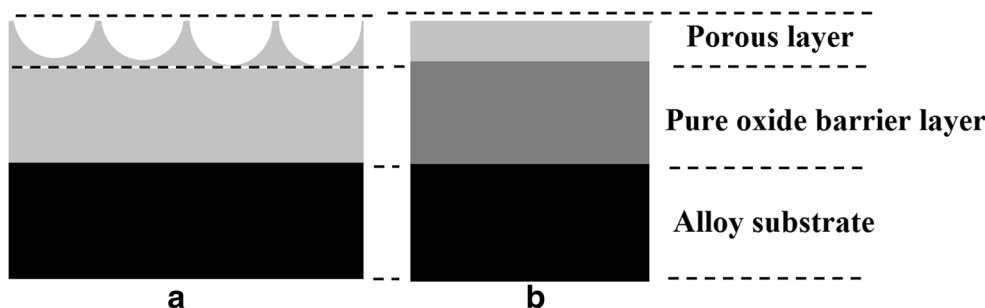
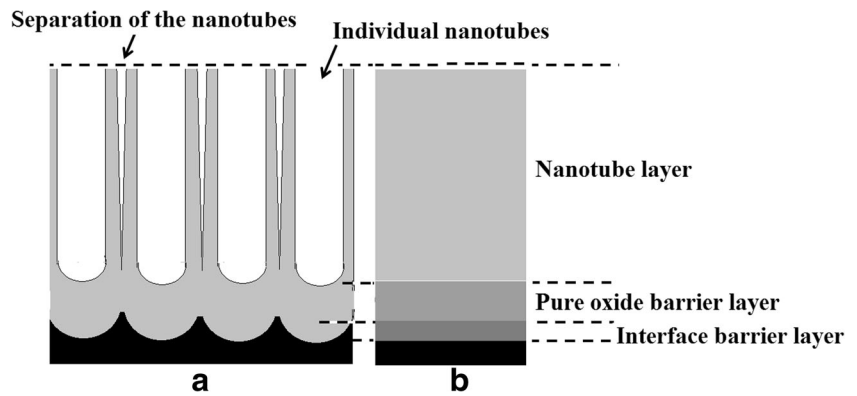


Fig. 4 **a** Morphology of the nanotubes anodic film after anodization at 20 V for 20 min; **b** optical model of (a) for SE interpretation



FEG-SEM (Fig 5). In our SE approach, the standard procedures consider the porosity to be uniform in all directions, but it is not the case here, leading to possible discrepancies.

The oxide film grown for 2 min was modeled with a double layer. In this film, the inner layer is compact while the outer one is rough with high void fraction. For 10 and 20 min, the model used considers three layers. The inner layer contains the substrate/oxide interface, which is modeled as an undulated interface. The middle layer is a compact oxide layer and the outer one represents the layer of titanium oxide nanotubes. In the optical model, pore and nanotube layers are characterized in the standard way [9, 17, 18] by a mixture of amorphous titanium oxide and voids. On the other hand, the substrate/oxide interface is represented by a mixture of substrate and oxide.

Table 1 presents the layers' thickness values and the fit parameters [R^2 and Root Mean Square Error ($RMSE$)] for the nanostructured films produced using different processing/anodizing times. The excellent fits obtained for our experimental data ($R^2 = 0.99$ and $RMSE \leq 0.02$) confirm the quality of our modeling.

The structure changes from a bi-layer film for 2 min growth time to a three-layer film for 10 min growth time. This change shows that the film undergoes a morphological transformation during the anodization process (Figs. 3 and 4 and Table 1).

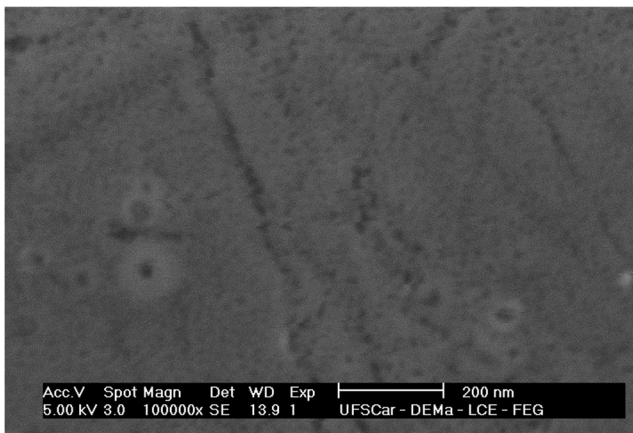


Fig. 5 Top view FEG-SEM image of the structure of TiO_2 films on Ti-6Al-7Nb alloy after anodization for 2 min

Figures 5 and 6, obtained by FEG-SEM, show the images of the structures formed with 2 and 20 min growth times, respectively. After anodization for 2 min, Fig. 5 shows that the surface of the 60-nm-thick film is rough. Figure 6a–c shows the top, cross-section, and the bottom-view images of the nanotubes of TiO_2 films on the alloy after anodization for 20 min. In Fig 6c, the oxide layer was inverted when the surface was scratched and the scalloped barrier film was revealed. These images show that the nanotubes' diameter and thickness values are close to 60 and 250 nm, respectively, in very good agreement with the optically determined thickness of about 217 nm, within the respective error and uncertainty limits of FEG-SEM and SE.

The void fraction shown in Table I, given by the SE model, was estimated from Fig. 6a, by image analysis. The voids are found in the interior regions of the nanotubes and regions between them. It is somewhat difficult to measure accurately these regions. In practical terms, the void fraction is identified as the ratio between the black and white pixels, given directly by ImageJ. We have obtained a crop of Fig. 6a where only the nanotube layer is present. By using the Huang and Otsu threshold algorithms [20], in the free software ImageJ [21] created by Wayne Rasband, we have binarized the gray level of the cropped image. A void fraction of 37.44 % is achieved, once gray level 66 is used as the threshold, calculated by the Huang algorithm. Using gray level 76, obtained by the Otsu

Table 1 Parameter values after regression for the nanostructured films formed in different times

Time		2 min	10 min	20 min
Porous/nanotube layer	Thickness (nm)	15	148	217
	Void fraction (%)	72	14	41
Barrier layer	Thickness (nm)	45	1	42
Interface layer	Thickness (nm)	–	3	80
	Oxide fraction (%)	–	90	88
Total thickness (nm)		60	152	339
R^2		0.99	0.99	0.99
$RMSE$		0.02	0.02	0.01

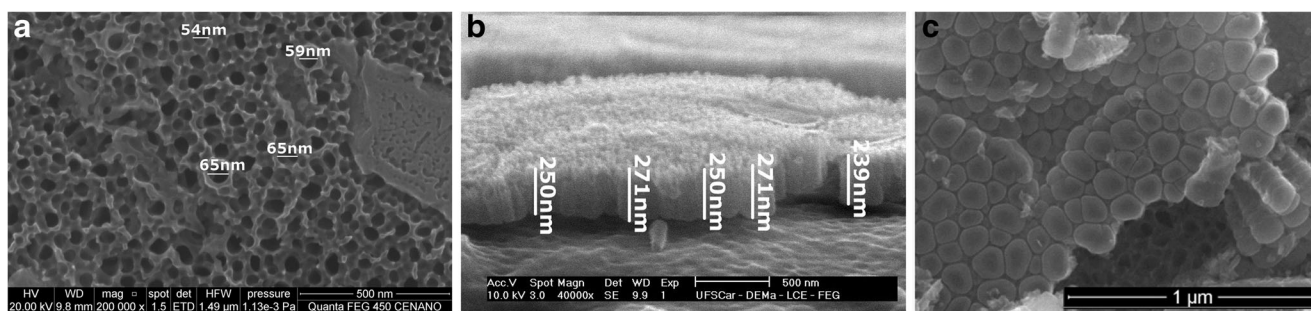


Fig. 6 Top (a), cross-section (b), and the bottom-view (c) FEG-SEM images of the structure of TiO₂ films on Ti-6Al-7Nb alloy after anodization for 20 min

algorithm, a void fraction of 55.79 % was obtained. The average of the results is 44.77 %. It is worth mentioning that the area of interest (nanotube layer) shown in Fig 6a is roughly 7.7 μm² while the microspot illuminated area of the ellipsometer is about 0.1 mm² (365 × 270 μm at 75°). So the variations shown in these percentages can be considered as fluctuations, since the analyzed region of the SEM image is much smaller than the area used for SE measurement and modeling; besides this, the pores do not have a homogeneous diameter distribution over the analyzed area. Considering this, these results are in good agreement with the 41 % void fraction obtained by our SE modeling.

From these results (Table 1 and Figs. 5 and 6), it is possible to propose a mechanism similar to the self-ordered nanotubular structure of anodic oxide layer formed on titanium [17], with the beginning of pore creation occurring after 2 min of anodization, and formation of nanotubes on the alloy at 20 min (Fig 7). As a consequence of the curvature and increased stress concentration at the valleys in the initial oxide surface on the alloy (Fig. 7a), the chemical potential would be higher than the values at the crests when the surface is sinusoidally perturbed. The ions could be preferentially adsorbed on the valleys as a result of the difference in chemical potentials. In order to maintain the electroneutrality, more H⁺ ions could migrate to these sites and lead to a dissolution of Ti⁴⁺ ions. Therefore, valleys dissolve preferentially and crests

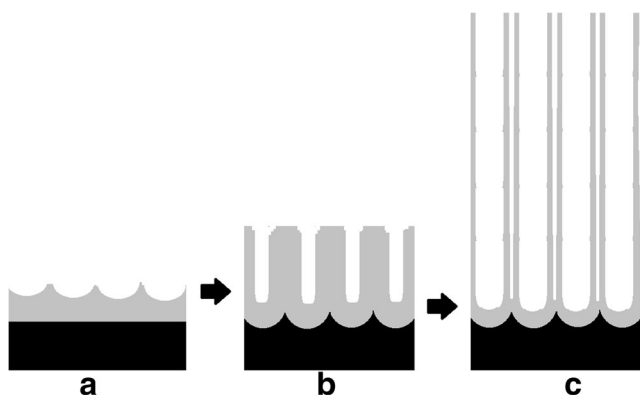


Fig. 7 Schematic diagram showing pore creation (a and b) and formation of nanotubes on anodized alloy (c)

grow at their expense leading to a self-ordered porous structure. We propose that void fraction decreases during the formation of the self-ordered porous structure (Fig. 7b). After this, the separation of individual nanotubes of the titanium oxide layer from the inter-connected nanopores occurs, and there is an increase in the void fraction and thickness of the outer layer (Fig. 7c).

We now discuss the results for the nanoindentation test. In Fig. 8, we present typical load and unload curves for the Ti-6Al-7Nb alloy substrate with air-formed oxide film (dashed line) and for the same substrate with TiO₂ nanotubes after anodization for 20 min with 20 V (solid line). As can be seen, the indentation depth in the nanotubes is much more accentuated ($h_{MAX} = 0.17 \pm 0.01 \mu\text{m}$) in comparison to the air-formed oxide film on the substrate ($h_{MAX} = 0.10 \pm 0.01 \mu\text{m}$). Using a Vickers indenter (DHV), the measured dynamical hardness with a for the nanotubes was $DHV_{NT} = 1153 \pm 399$, and for the air-formed oxide film on the substrate, it was $DHV_S = 2,327 \pm 198$, as expected, since it is due to the higher indentation depth in the film with nanotubes compared to the ones of the substrate. After penetration in the film surface, the indentation occurs along the nanotubes producing shear forces during the

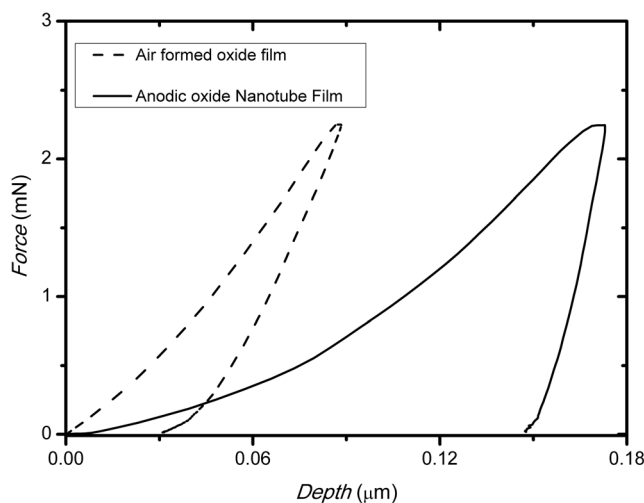


Fig. 8 Load–unload curve for the substrate Ti-6Al-7Nb (dashed line) and for the TiO₂ nanotubes produced with Ti-6Al-7Nb after anodization for 20 min with 20 V (solid line)

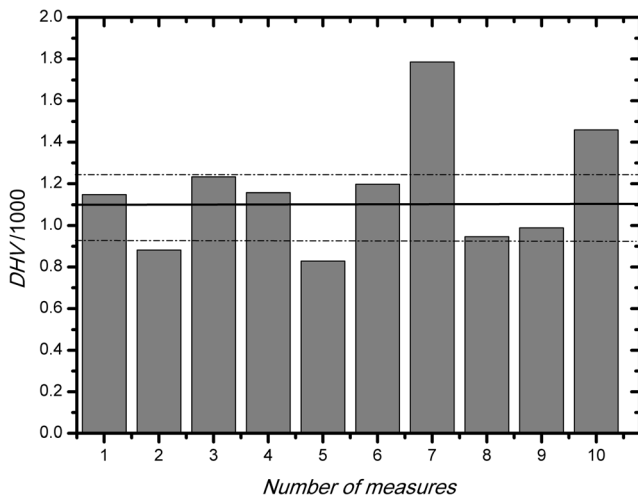


Fig. 9 Measurement of the hardness DHV for 10 different regions of the sample. The *solid line* shows the limit border between the two distinct groups $DHV > 1100$ and $DHV < 1100$. The *upper dashed line* is the mean value for DHV of the group with $DHV > 1100$ and the *lower dashed line* is the same for the group with $DHV < 1100$

indenter's descent, which can probably separate and even break the nanotubes, contributing to a lowering of the hardness. Note that h_{MAX} for the film with nanotubes is of the order of half of the nanotubes' extension (layer thickness). Considering the elasticity, we can observe that the film with nanotubes presents a larger-area load-unload curve, which means that the elastic restitution is worse than that of the substrate.

Considering the two possible phases (α and β), the mechanical properties of Ti-6Al-7Nb alloy surfaces may be modified due to the presence of biphasic regions after anodization [5, 7]. Concerning the random superficial distribution of the α and β phases, after 10 measurements, we found a high deviation for the DHV value (around 40 %) for the oxide with nanotubes. Figure 9 shows the results from 10 measurements of the DHV on different regions of the sample's surface. We can observe two distinct groups of results, i.e., above and below $DHV = 1100$, represented by the solid line. The upper dashed line is the mean value of the hardness above $DHV = 1100$, while the lower dashed line represents the mean value of the hardness DHV below 1100. The difference between these two averages is in agreement with the deviation of the mean values. It can be a signature of the effect of the α and β phases on the hardness of the anodized surface.

Conclusions

In summary, TiO₂ nanotube layers were obtained by using the single-step direct anodization of Ti-6Al-7Nb alloy in aqueous electrolytes containing F⁻ ions. The grown oxide film is modeled using SE. The obtained results present an excellent fitting and are in very good agreement with FEG-SEM

analysis. Nanoindentation showed a lowering of the surface hardness with the presence of TiO₂ nanotube layers. In future work, we will perform a SE study “in situ”, during the nanotube layer formation, which will require a complete characterization of the end point of the anodization process. These results should provide a better understanding of the dynamics of layer growth.

Acknowledgments The authors thank the funding agencies FINEP, CNPq, PROPP/UFF, and FAPERJ (Process E-26/111.368/2014) for financial support, and PhD Erika Batista Silveira and INT for technical assistance during the electron microscopy analyzes. The authors are in debt with Urszula Mieñkowska Verissimo and Marcos Verissimo Alves for the revision of the manuscript.

References

- Stepień M, Handzlik P, Fitzner K (2014) Synthesis of ZrO₂ nanotubes in inorganic and organic electrolytes by anodic oxidation of zirconium. *J Solid State Electrochem* 18:3081–3090
- Fang D, Yu J, Luo Z, Liu S, Huang K, Xu W (2012) Fabrication parameter-dependent morphologies of self-organized ZrO₂ nanotubes during anodization. *J Solid State Electrochem* 16:1219–1228
- Hahn R, Berger S, Schmuki P (2010) Bright visible luminescence of self-organized ZrO₂ nanotubes. *J Solid State Electrochem* 14:285–288
- Roy P, Berger S, Schmuki P (2011) TiO₂ nanotubes: synthesis and applications. *Angew Chem Int* 50:2904–2939
- Nguyen TT, Park I-S, Lee MH, Bae TS (2013) Enhanced biocompatibility of a pre-calcified nanotubular TiO₂ layer on Ti-6Al-7Nb alloy. *Surf Coat Tech* 236:127–134
- Almeida LC, Zanoni MVB (2014) Decoration of Ti/TiO₂ nanotubes with Pt nanoparticles for enhanced UV-Vis light absorption in photoelectrocatalytic process. *J Braz Chem Soc* 25:579–588
- Macak JM, Tsuchiya H, Luciano TL, Ghicov A, Schmuki P (2005) Self-organized nanotubular oxide layers on Ti-6Al-7Nb and Ti-6Al-4 V formed by anodization in NH₄F solutions. *Inc J Biomed Mater Res* 75A:928–933
- Rafieerad AR, Zalnezhadha E, Bushroa AR, Hamouda AMS, Sarraf M, Nasiri-Tabrizi B (2015) Self-organized TiO₂ nanotube layer on Ti-6Al-7Nb for biomedical application. *Surf Coat Tech* 265:24–31
- Joo S, Muto I, Hara N (2008) In situ ellipsometric analysis of growth processes of anodic TiO₂ nanotube films. *J Electrochem Soc* 155:C154–C161
- Cáceres D, Munuera C, Ocal C, Jiménez JA, Gutiérrez A, López MF (2008) Nanomechanical properties of surface-modified titanium alloys for biomedical applications. *Acta Biomater* 4:1545–1552
- Fujiwara H (2007) Spectroscopic ellipsometry principles and applications. John Wiley & Sons Ltd, England
- Irena LJ, Arsova IL, Prusi AR, Arsov LD (2003) Ellipsometric study of anodic oxide films formed on niobium surfaces. *J Solid State Electrochem* 7:217–222
- Crawford GA, Chawla N, Das K, Bose S, Bandyopadhyay A (2007) Microstructure and deformation behavior of biocompatible TiO₂ nanotubes on titanium substrate. *Acta Biomater* 3:359–367
- Ibarra YS, Gaitero JJ, Erkizia E, Campiolo I (2006) Atomic force microscopy nanoindentation of cement pastes with nanotubes dispersions. *Phys Stat Sol* 203:1076–1081

15. Campanelli LC, Duarte LT, da Silva PSCP, Bolfarini C (2014) Fatigue behavior of modified surface of Ti-6Al-7Nb and CP-Ti by micro-arc oxidation. *Mater Design* 64:393–399
16. Duarte LT, Bolfarini C, Biaggio SR, Rocha-Filho RC, Nascente PAP (2014) Growth of aluminum-free porous oxide layers on titanium and its alloys Ti-6Al-4 V and Ti-6Al-7Nb by micro-arc oxidation. *Mater Sci Eng C* 41:343–348
17. Raja KS, Misra M, Paramguru K (2005) Formation of self-ordered Nano-tubular structure of anodic oxide layer on titanium. *Electrochim Acta* 51:154–165
18. Laet J, Terryn H, Vereecken J (1998) Development of an optical model for steady state porous anodic films on aluminum formed in phosphoric acid. *Thin Solid Films* 320:241–252
19. Hebert KR, Albu SP, Paramasivam I, Schmuki P (2012) Morphological instability leading to formation of porous anodic oxide films. *Nat Mater* 11:162–166
20. Advanced shape analysis with ImageJ (2008) Proceedings of the Second ImageJ User and Developer Conference, Luxembourg. <http://www.mecourse.com/landinig/software/software.html> Accessed 06 Jan 2015
21. ImageJ, Image processing and Analysis in Java (2004) National Institutes of Health, United States. <http://imagej.nih.gov/ij/index.html> Accessed 06 Jan 2015